Materials Characterization 144 (2018) 219–226

Contents lists available at ScienceDirect

Materials Characterization

journal homepage: www.elsevier.com/locate/matchar

Crystallography of intergranular corrosion in sensitized austenitic stainless steel

Tomoyuki Fujii*, Keiichiro Tohgo, Yota Mori, Yoshinobu Shimamura

Department of Mechanical Engineering, Shizuoka University, 3-5-1, Johoku, Naka-ku, Hamamatsu 432-8561, Japan

ARTICLE INFO

Keywords:
Intergranular corrosion
Grain boundary
Grain boundary character
Coincidence site lattice
Misorientation

ABSTRACT

This study deals with the susceptibility to intergranular corrosion (IGC) in type 304 austenitic stainless steel from a crystallographic viewpoint. An IGC test was conducted using oxalic acid and sensitized stainless steel, whose crystal orientation was analyzed by electron backscattered diffraction (EBSD). GBs were classified according to the misorientation of adjacent grains, and subclassified using the Σ value based on the coincidence site lattice (CSL) model. The width of corroded groove was measured for each GB category, and the effect of GB category on the susceptibility to IGC was examined. Then, the area of the unit cell of CSL boundaries was used to characterize the susceptibility to IGC of CSL boundaries. It was found that no IGC occurred in low-angle GBs with a misorientation of $< 10^{\circ}$, while IGC occurred in some of the low-angle GBs with misorientations of 10°–15°. In large-angle GBs with misorientations of $> 15^{\circ}$, the width of corroded groove at each Σ boundary exhibited large scatter. The relationship between the width and unit cell area was characterized by a sigmoid curve, and the susceptibility to IGC was well described by the unit cell area.

1. Introduction

Austenitic stainless steels have been attracting attention because of their high mechanical performance and corrosion resistance over a wide temperature range. They are widely used for many applications in various industries, such as tableware, medical implants, pipes, exhaust headers, and pressure vessels. If they are exposed to elevated temperature during welding, etc., chromium carbide precipitation and chromium depletion occurs at grain boundaries (GBs) (so-called sensitization). This results in the deterioration of GB corrosion properties [1–4] and unexpected failure due to intergranular corrosion (IGC) and intergranular stress corrosion cracking (IGSCC). A number of approaches have been followed to avoid sensitization and to improve the corrosion resistance of GBs. One such approach is to change the chemical composition of the steel: the chromium and/or nickel content and carbon content is increased and decreased, respectively, to avoid chromium depletion [5,6]. Another approach is to use a grain boundary engineering concept based on controlling the grain size and grain boundary character distribution (GBCD) [7–14]. It is well known that there are some special GBs with periodic atomic structure [15]. The structure of the special GBs is generally discussed on the basis of the coincidence site lattice (CSL) model, and is described by the Σ value, which is defined as the reciprocal of the density of coincidence sites [16]. The special GBs are referred to as the CSL or Σ boundaries. It is expected that low-Σ boundary exhibit high IGC resistance because lower-Σ boundary has a lower GB energy. Hence, a thermomechanical treatment has been proposed to increase the fraction of low-Σ boundaries. Wang et al. [9] fabricated type 316L austenitic stainless steel by controlling the GBCD, and evaluated its IGC and IGSCC resistance. Increasing the fraction of low-Σ boundaries was found to be effective in improving the IGC and IGSCC resistance of the steel. Shimada et al. [10], Hu et al. [11], Kobayashi et al. [12], Chen et al. [13], and Barr et al. [14] similarly demonstrated the effectiveness of controlling the GBCD for improving the IGC resistance of austenitic stainless steels.

Many studies have been conducted to investigate the influence of GB character on the susceptibility to IGC and IGSCC in austenitic stainless steels [17–21]. These studies revealed that lower-Σ boundaries, in particular, the Σ3 boundary, tended to exhibit IGC and IGSCC resistance. However, Gertsman et al. [20] suggested that other factors might affect the corrosion resistance of GBs, as IGSCC occurred at some lower-Σ boundaries, including the Σ3 boundary. Note that the crystallographic investigations by Gertsman et al. were based on an analysis by electron backscattered diffraction (EBSD), and experimental data related to the susceptibility to IGC and IGSCC showed wide scatter. The influence of the susceptibility of the Σ value has been investigated using statistical data, such as the ratio of IGC and IGSCC length to total GB

* Corresponding author.
E-mail address: fujii.tomoyuki@shizuoka.ac.jp (T. Fujii).

https://doi.org/10.1016/j.matchar.2018.07.014
Received 17 May 2018; Received in revised form 11 July 2018; Accepted 12 July 2018
Available online 17 July 2018
1044-5803/

length. This means that the use of the Σ value, as measured by EBSD, is insufficient to elucidate the criteria of IGC and IGSCC occurrence at GBs. Haruna et al. [19] pointed out the fundamental uncertainties related to EBSD measurements and discussed the susceptibility to IGC on the basis of the correct GB structure of several Σ3 boundaries detected in type 304 stainless steel. It is expected that the susceptibility can be characterized in detail in terms of a parameter describing the geometric features of GBs, in addition to the Σ value.

The aim of this study is to elucidate the susceptibility to IGC in austenitic stainless steels from a crystallographic viewpoint. IGC testing was conducted under a constant current in oxalic acid, and the width of the corroded groove, which occurred at GBs, was measured. Prior to testing, the crystal orientation was analyzed by EBSD, and the relationship between the width and crystallographic parameters, such as the misorientation and the Σ value, was discussed. Then, in order to determine the susceptibility to IGC in large-angle GBs with a misorientation of > 15°, a parameter was proposed that can characterize the geometric features of CSL boundaries.

2. Experimental

2.1. Material

Type 304 austenitic stainless steel was used. Table 1 shows the chemical composition of the steel. The steel was solutionized by heat treatment at 1100 °C for 1 h, and then sensitized by heat treatment at 700 °C for 2 h and 500 °C for 24 h. The average grain diameter of the steel was 119 μm, which was measured through the line-intercept method in accordance with Japanese Industry Standard (JIS) G 0551. The reactivation ratio of the steel was 29.3%, which was measured by the electrochemical potentiokinetic reactivation technique in accordance with JIS G 0580. Note that the reactivation ratio is defined as the ratio of reactivation peak current density to activation peak current density based on a reciprocating anodic polarization curve of the steel in a sulfuric acid solution containing potassium thiocyanate.

A 20 × 14 × 5 mm specimen was machined from bulk material after heat treatment. Its surface was ground with emery paper up to #2000, and then polished with diamond paste with 3 μm grain diameter and colloidal silica (OP-U, Marumoto Struers K.K.). For corrosion testing, a conductive wire was connected to the specimen, and all its surfaces, except for a 10 × 10 mm etching area, were coated with plastic for insulation, as shown in Fig. 1.

2.2. Crystallography

Prior to corrosion testing, the crystal orientation of the etching area was measured with an EBSD system (Orientation imaging microscopy, TSL Solutions) installed in a field-emission SEM (JSM-7001F, JEOL Ltd). The specimen was placed at a 70° incline with respect to the detector, and the specimen coordinate system was set to be the long direction (x^P), short direction (y^P), and normal direction to the specimen surface (z^P), as shown in Fig. 1. Measurement data were acquired and analyzed with OIM data correction and OIM analysis (TexSEM), respectively. Table 2 tabulates the EBSD measurement conditions. Fig. 2(a) and (b) show, respectively, the map of crystal orientation normal to the specimen surface and the specimen surface corresponding to (a) after etching.

The crystal orientation at each measurement site was measured using the Euler angle (ϕ_1, Φ, ϕ_2) defined by Bunge [22]. The orientation

Table 1
Chemical composition of type 304 austenitic stainless steel (mass%).

C	Si	Mn	P	S	Ni	Cr	Fe
0.06	0.47	0.87	0.03	0.003	8.05	18.16	Bal.

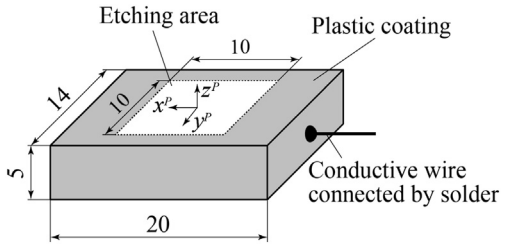

Fig. 1. Specimen dimensions (in units of mm) and experimental setup.

Table 2
Conditions of EBSD measurement and analysis using OIM.

Grid shape	Hexagonal
Measurement interval, μm	3.5
Grain tolerance angle, deg.	5
Minimum grain size, pixel	2
Clean up	Grain dilation, single iteration

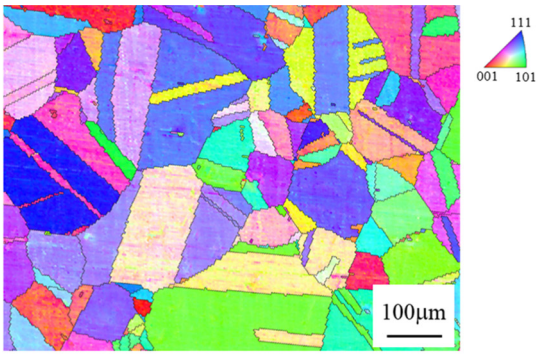

(a) Crystal orientation map of specimen surface before etching. Black lines denote GBs whose misorientations range from 5° to 180°.

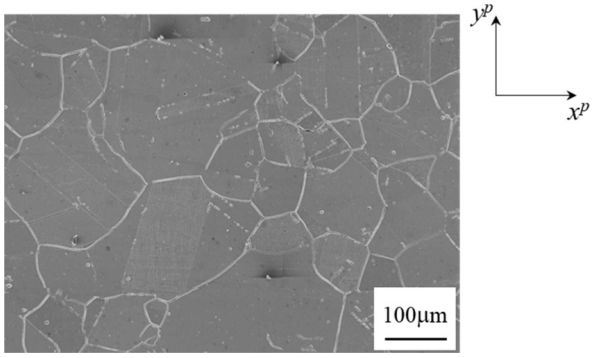

(b) SEM image of specimen surface etched with oxalic acid.

Fig. 2. Microstructure of the sensitized stainless steel specimen used.

matrix **M** is given by

$$\mathbf{M} = \begin{bmatrix} \cos\phi_1\cos\phi_2 - \sin\phi_1\sin\phi_2\cos\Phi & \sin\phi_1\cos\phi_2 + \cos\phi_1\sin\phi_2\cos\Phi & \sin\phi_2\sin\Phi \\ -\cos\phi_1\cos\phi_2 - \sin\phi_1\cos\phi_2\cos\Phi & -\sin\phi_1\sin\phi_2 + \cos\phi_1\cos\phi_2\cos\Phi & \cos\phi_2\sin\Phi \\ \sin\phi_1\sin\Phi & -\cos\phi_1\sin\Phi & \cos\Phi \end{bmatrix} \quad (1)$$